HHS Public Access

Author manuscript

AAPS J. Author manuscript; available in PMC 2023 May 15.

Published in final edited form as:

AAPS J. ; 25(3): 29. doi:10.1208/s12248-023-00799-1.

Development of Drug Release Model for Suspensions in ESCAR (Emulator of SubCutaneous Absorption and Release)

Hao Lou[1,2], **Michael J. Hageman**[1,2]

[1]Department of Pharmaceutical Chemistry, University of Kansas, Lawrence, KS 66047, USA

[2]Biopharmaceutical Innovation and Optimization Center, University of Kansas, Lawrence, KS 66047, USA

Abstract

We recently developed an *in vitro* testing system, namely, ESCAR (Emulator of SubCutaneous Absorption and Release). The objective of this work was to investigate drug release behaviors of unmilled and milled suspensions in ESCAR. A mass transport-based model was developed to describe the multi-step drug release process, including drug dissolution, particle settling, drug distribution/partition, and drug permeation through the membrane(s). To address the particle settling effect, a correction factor was included in the model and its value was obtained by data fitting. It was found that, for both suspensions, (i) the experimental data of various dose/formulation combinations could be fit by the developed model; (ii) the dose effect on drug release was offset by the particle settling effect. This model may help to reduce experimental efforts and facilitate subcutaneous suspension formulation development using ESCAR.

Keywords

drug release; *in vitro* system; mass transport; subcutaneous route of administration; suspension

Introduction

For small molecule drug delivery, despite the prevalence of the oral route of administration, many drug products are administered via the subcutaneous (SC) route for human and veterinary uses (1). SC administration provides several advantages such as (i) the avoidance of hepatic first-pass metabolism; (ii) a suitable route for long-acting and extended-release formulations; (2, 3) (iii) an alternative route for patients who are difficult to use the oral intake or molecules that are incompatible with the gastrointestinal environment; (iv) a possible low peak-to-trough ratio of pharmacokinetics (PK) profile and therefore the

✉ Hao Lou, lou0@ku.edu, Michael J. Hageman, mhageman@ku.edu.

Authors' Contributions H.L. contributed to conceptualization, methodology, software, formal analysis, writing—original draft, visualization, and project administration. M.J.H. contributed to writing—review and editing, project administration, supervision, and resources. All authors read and approved the final manuscript.

Conflict of Interest The authors declare that they have no conflicts of interest.

Supplementary Information The online version contains supplementary material available at https://doi.org/10.1208/s12248-023-00799-1.

potential improvement of drug tolerability; (4) (v) the capability of implementing wearable drug delivery devices (4, 5).

Since the SC injection volume is typically less than 1.5 mL (6) and many small molecules possess low water solubility, one remarkable advantage of a suspension formulation is that it can obtain higher doses compared to a solution formulation. In addition, some drugs may have better stability in suspension than in solution (1). Some authorized small molecule drug products formulated as suspension for SC administration include azacytidine (human use), leuprorelin (human use), and ceftiofur (veterinary use) (1). Small molecule drugs can also be formulated as nanosuspension for SC administration, and some PK studies on rodents report that nanosuspension most often exhibits higher systemic exposure compared to microsuspension (7–11). These results suggest the potential clinical benefits of nanosuspension, although currently there are no reliable models which can translate rodent data to other animal species as well as human beings (12). Unfortunately, SC formulation (e.g., suspension) development can be impeded by unpredictable and variable PK profiles due to inter-species and inter-subject differences in the SC environment and drug uptake pathways (13, 14). Furthermore, animal testing is not the most economical approach and is inconsistent with the 3R (replacement, reduction, and refinement) principle. Therefore, there is a need to develop an *in vitro* testing system that can fit one or more of the following purposes: (i) to apply as a routine quality control method to assess suspensions from different batches; (ii) to aid in SC suspension formulation screening and development; (iii) to establish an *in vitro-in vivo* correlation (IVIVC) method to waive some *in vivo* studies and/or support bioequivalence studies.

Since the conventional dissolution apparatuses such as USP Apparatus 1 and 2 are not suitable for testing SC formulations, researchers have made efforts to develop new *in vitro* systems that are more biorelevant to the SC environment, including dispersion releaser (15, 16). SC injection site simulator (SCIS-SOR), (17, 18) flow-through cell-based setup, (19) gel (e.g., agarose gel)-based setup (20) etc. These systems are designed to emulate some aspects of animal/human SC physiology. Strikingly, dispersion releaser and a gel matrix-packed flow-through cell-based setup are successfully applied to develop IVIVC models for SC formulations (15, 16, 19). In addition, a variety of release media are developed to simulate the SC interstitial fluid. (21) None of the aforementioned devices and media have been recommended by regulatory agencies as standard methods for *in vitro* testing of SC suspensions (12).

We recently developed an *in vitro* system, namely, ESCAR (Emulator of SubCutaneous Absorption and Release), and employed it to assess suspension formulations with the establishment of an IVIVC model (22). In our previous study, griseofulvin was formulated into both unmilled and milled suspensions, and drug release tests were carried out in ESCAR (22). In this study, we aim to further understand the drug release of the developed unmilled and milled suspensions at different doses using both the experimental and modeling approaches. Drug release tests of various formulation/dose combinations were conducted. Furthermore, a mass transport-based model was developed, and the best-fit values of the corresponding parameters were obtained by data fitting.

Modeling: Drug Release in ESCAR

Because the ESCAR geometry (shown in Fig. 1) is symmetrical and the same experimental conditions are utilized for both "blood circulation" chambers, these two chambers can be treated as one compartment in our proposed model. Therefore, the "SC" chamber is assigned as Compartment 1 and the "blood circulation" chambers are assigned as Compartment 2. For drug release model development, some assumptions are made as follows.

- **i.** In Compartment 1, the dissolved drug molecules diffuse rapidly in the aqueous phase and instantaneously reach an equilibrium between the aqueous phase and the oil phase. It is worth mentioning that the aqueous phase reflects the SC interstitial fluid, and the oil phase reflects the adipose tissue and skin lipid.
- **ii.** In Compartment 1, there exists a partition constant (k_P) between the aqueous (continuous) phase and the oil (dispersed) phase.
- **iii.** Only drug molecules in the aqueous phase can permeate through the membrane.
- **iv.** Throughout the drug release process, since the concentration in Compartment 2 (Conc2) is extremely low, it is acceptable to use zero for Conc2 for model development.
- **v.** By combining assumptions (iii) and (iv), the concentration gradient of the two compartments is equal to the aqueous phase concentration in Compartment 1 (Conc1).
- **vi.** At the beginning of drug release tests, all particles in the suspension are spherical and have an equal particle size (Dia_0).
- **vii.** To simplify the model, as dissolution proceeds, particle size is assumed to decrease at the same rate across all particles. Hence, all particles have an equal particle size during the drug release process.

According to assumption (v), the change in drug amount in Compartment 2 is expressed by Eq. 1.

$$\frac{d(\mathrm{Amt2})}{\mathrm{dt}} = \mathrm{SA}_{\mathrm{permeation}} \times k_{\mathrm{mem}} \times \mathrm{Conc1} \tag{1}$$

where Amt2 is the total drug amount in Compartment 2, $\mathrm{SA}_{\mathrm{permeation}}$ is the total surface area available for drug permeation, k_{mem} is permeability constant that can be determined by experiments (the method is listed in "Membrane permeation tests to determine k_{mem}" section).

According to assumption (ii), there exists a distribution volume (V_d), which can be expressed by Eq. 2.

$$V_d = k_p \times V_p \tag{2}$$

where V_p is the physical volume of the "SC" chamber, and k_P is partition constant that can be determined by experiments (the method is listed in "Membrane flux tests to determine kP" section).

Next, the change of the aqueous phase concentration in Compartment 1 (Conc1) and particle size (Dia) can be expressed by Eqs. 3 and 4, respectively.

$$\frac{d(\text{Conc1})}{dt} = \left[\text{CF}_{(t,\text{Dia},\text{Dose})} \times \frac{\text{DC}}{H}\left(\pi \times \text{Dia}^2\right)N_0(C_s - \text{Conc1}) - \text{SA}_{\text{permeation}} \times k_{\text{mem}} \times \text{Conc1}\right]/V_d \quad (3)$$

$$\text{Dia} = \sqrt[3]{\frac{(\text{Dose} - \text{Conc1} \times V_d - \text{Amt2})/N_0}{\rho\pi/6}} \quad (4)$$

Assuming that there is a diffusion layer for particle dissolution, DC represents drug diffusion coefficient, H represents diffusion layer thickness, C_s represents drug solubility, and ρ is drug particle density. In addition, N_0 is the total number of particles, which can be calculated by Eq. 5.

$$N_0 = \frac{6 \times \text{Dose}}{\rho\pi(\text{Dia}_0)^3} \quad (5)$$

Furthermore, due to the lack of agitation in the "SC" chamber, particles tend to settle over time. In consequence, the total surface area available for particle dissolution is less than the theoretical surface area which is $\left(\pi \times \text{Dia}^2\right)N_0$. To reflect the particle settling effect, a correction factor CF is added to Eq. 3, and CF is a factor with its value related to time, particle size, and dose. Since DC and H are two constants, $CF_{(t,\text{Dia},\text{Dose})} \times \frac{DC}{H}$ can be replaced by a new term $Q_{(t,\text{Dia},\text{Dose})}$, and Eq. 3 can be rewritten to Eq. 6.

$$\frac{d(\text{Conc1})}{dt}/V_d = \left[Q_{(t,\text{Dia},\text{Dose})} \times \left(\pi \times \text{Dia}^2\right)N_0(C_s - \text{Conc1}) - \text{SA}_{\text{permeation}} \times k_{\text{mem}} \times \text{Conc1}\right] \quad (6)$$

The values of the above-mentioned parameters (listed in Table II) can be either obtained from literature or determined by experiments. In terms of the initial condition, the initial particle size (Dia_0) was 1.5 μm for the milled suspensions, and 26.2 μm for the unmilled suspensions; the initial aqueous phase concentration in Compartment 1 (Concl_0) was 0.636 μg/mL. Via fitting the experimental data and solving Eqs. 1, 4, and 6 numerically using the codes programmed in MATLAB R2018a (MathWorks, MA, USA), the best-fit values of $Q_{(t,\text{Dia},\text{Dose})}$ can be obtained.

Materials and Methods

Materials

ABSplus white and SR-30 were purchased from Stratasys (Edina, MN, USA). Griseofulvin (97.0 to 102.0%) and Tween®80 were purchased from Sigma-Aldrich (St. Louis, MO, USA). Hyaluronic acid (average MW: 1.64 mDa) was purchased from Lifecore Biomedical, Inc (Chaska, MN, USA). SpectraPor regenerated cellulose dialysis membrane (50 kDa MWCO) and lecithin (90% soybean) were purchased from Fisher Scientific (Ward Hill, MA, USA). All solvents utilized in the present study were HPLC analytical grades.

Unmilled and Milled Suspension Preparation

A series of unmilled and milled suspensions of various drug contents were prepared. The preparation procedures were described as follows.

An unmilled suspension was prepared by adding a pre-calculated amount of griseofulvin bulk powder in 1.5 mL of 0.5% Tween® 80 (w/w) PBS, followed by 5-min sonication.

A milled suspension was prepared via a wet milling method. Griseofulvin bulk powder, as well as 0.5-mm zirconium beads, were loaded in a scintillation vial. Sequentially, a certain volume of 0.5% Tween® 80 (w/w) PBS was added to reach the drug concentration of suspension at 50 mg/mL. The suspension was wet milled at 1200 rpm using a magnetic stir bar for 24 h with intermittent shaking.

Mastersizer 3000 particle size analyzer (Malvern Panalytical, MA, USA) was applied to characterize unmilled suspensions, and Zetasizer (Malvern Panalytical, MA, USA) was utilized to characterize milled suspensions. A variety of concentrations were prepared by diluting the prepared milled suspension (50 mg/mL) with 0.5% Tween® 80 (w/w) PBS at pre-calculated ratios.

Suspension Settling Tests

Both unmilled and milled suspensions tended to settle under gravity. A turbidity test was conducted to evaluate particle settling versus time using a Varian Cary® 50 UV–Vis spectrophotometer (Agilent Technologies, CA, USA) at ambient temperature. For turbidity measurement, the unmilled suspension was prepared at 2 mg/mL, and the milled suspension was prepared at 0.5 mg/mL. Briefy, 700 μL of the well-shaken suspension was filled in a Beckman Quartz micro cuvette cell (10-mm pathlength). Next, the cuvette cell was immediately inserted into the cuvette holder and placed there stationarily during the test. At each time point, the absorbance was measured at 500 nm. For each suspension, the turbidity test was conducted in triplicate.

Griseofulvin Quantification Using HPLC

Griseofulvin concentration was quantified using a Shimadzu HPLC system (Shimadzu Corporation, Kyoto, Japan) installed with an XBridge™ C18 column (3.5 μm, 4.6 mm × 150 mm) at 291 nm UV detection wavelength. The mobile phase consisted of 35% (v/v) of 0.1% trifluoroacetic acid in water (mobile phase A) and 65% (v/v) of acetonitrile (mobile

phase B). The flow rate was kept at 1 mL/min. Both the column chamber and the detector chamber were maintained at 40 °C.

Membrane Permeation Tests to Determine k_{mem}

A side-by-side cell (PermeGear, PA, USA) was used for membrane permeation tests. The donor and receiver cells with a volume of 10 mL and an orifice diameter of 15 mm were separated by a SpectraPor® dialysis membrane (MWCO 50 kDa) and tightened by an adjusting knob. Prior to the tests, the membranes were pre-soaked in DI water for at least 1 h, and the medium and drug solution were pre-warmed in a 34 °C water bath. To begin the tests, the receiver cell was filled with 10 mL of PBS (pH 7.4) and the donor cell was filled with 10 mL of the solution of griseofulvin and PBS (~ 3.3 μ g/mL). The experiments were conducted at 34 °C with magnetic stirring in both cells. At each time point, 100 μ L of aliquots were withdrawn from both cells for concentration quantification. The permeability constant k_{mem} could be determined by Eq. 7.

$$k_{\text{mem}} = \frac{\text{DC}_{\text{mem}} \times \text{PC}_{\text{mem/aq}}}{H_{\text{mem}}} = \frac{1}{\Delta t \times \text{SA}_{\text{mem}} \times \left(\frac{1}{V_{\text{donor}}} + \frac{1}{V_{\text{receiver}}}\right)} \times \ln \left(\frac{\text{Conc}_{\text{donor}}^{t1} - \text{Conc}_{\text{receiver}}^{t1}}{\text{Conc}_{\text{donor}}^{t2} - \text{Conc}_{\text{receiver}}^{t2}}\right) \tag{7}$$

where DC_{mem} was drug diffusion coefficient in the membrane, $PC_{mem/aq}$ was the partition coefficient between the membrane and the liquid, H_{mem} was membrane thickness, SA_{mem} was the orifice area, Δt was the interval between the time points, and V_{donor} and $V_{receiver}$ were the liquid volume in the donor and receiver (10 mL was used with the neglect of subtle volume change due to aliquot sampling).

Membrane Flux Tests to Determine k_P

To characterize drug partition in the dispersed oil phase at a fixed percentage (1.64% w/v lecithin used in this study), membrane flux studies were performed. The same devices and materials used in “Membrane Permeation Tests to Determine k_{mem}” section were also utilized in “Membrane Flux Tests to Determine k_P” section The tests were undertaken at 34 °C with magnetic stirring in both cells.

For the first group, the receiver cell was filled with 10 mL of PBS (pH 7.4) and the donor cell was filled with 10 mL of griseofulvin-contained (~3.15 μg/mL) 1-mg/mL HA/PBS solution. Based on the results of the membrane permeation study (Sect. 4.2), it was acceptable to set the concentration in the donor cell ($Conc_{donos}$) constant throughout the experiment. Hence, the change of drug amount in the receiver cell $d(Amt_{receiver})/dt$ could be expressed by Eq. 8.

$$J_{\text{HA|PBS\_in\_donor}} = \frac{d(\text{Amt}_{\text{receiver}})}{dt}/\text{SA}_{\text{mem}} = k_{\text{mem}} \times \text{Conc}_{\text{donor}} = k_{\text{mem}} \times \left(\frac{\text{Amt}_{\text{donor}}}{V_{\text{donor}}}\right) \tag{8}$$

For the second group, the receiver cell was filled with 10 mL of PBS (pH 7.4). The donor cell was filled with an emulsion prepared as follows: 10 mL of the griseofulvin-contained 1-mg/mL HA/PBS solution (the same solution as that used for the first group) was prepared and then mixed with the precalculated amount of lecithin (1.64% w/v). Therefore, there were the same amounts of griseofulvin in the donor cells of the first and second groups. For the second group, the change of drug amount in the receiver cell $d(\mathrm{Amt}_{\mathrm{receiver}})/dt$ could be expressed by Eq. 9.

$$J_{\mathrm{Lecithin|HA|PBS\_in\_donor}} = \frac{d(\mathrm{Amt}_{\mathrm{recevicere}})}{dt}/\mathrm{SA}_{\mathrm{mem}} = k_{\mathrm{mem}} \times \mathrm{Conc}_{\mathrm{donor\_aqueous\_phase}} = k_{\mathrm{mem}} \times \left(\frac{\mathrm{Amt}_{\mathrm{donor}}}{k_p \times V_{\mathrm{donor}}}\right) \quad (9)$$

Next, k_P could be calculated using Eq. 10. For both groups, the experiments were carried out in triplicate.

$$k_p = \frac{J_{\mathrm{HA|PBS\_in\_donor}}}{J_{\mathrm{Lecithin|HA|PBS\_in\_donor}}} \quad 10$$

ESCAR Design and Fabrication

The design and fabrication of ESCAR were described in detail in our previous paper (22). Briefly, ESCAR was designed with the aid of AutoCAD (Autodesk Inc., CA, USA) and fabricated by a Mojo 3D printer (Stratasys, Inc., MN, USA) followed by a series of post-printing procedures. ABSplus™ white was used as the printing material and SR-30™ was used as the soluble support material. ESCAR consisted of three chambers: one “SC” chamber at the center, and two “blood circulation” chambers on the left and right sides. The “SC” chamber, as seen in Fig. 1, had a dimension of 3 cm in length × 2.5 cm in height × 1 cm in width and two open windows (length 3 cm; height 2.5 cm; surface area 7.5 cm^2). The “blood circulation” chamber had an open window (length 3 cm; height 2.2 cm; surface area 6.6 cm^2). Therefore, the total surface area available for drug permeation ($\mathrm{SA}_{\mathrm{permeation}}$) was 13.2 cm^2 (6.6 cm^2 × 2).

Drug Release Tests in ESCAR

To conduct drug release tests in ESCAR, for each “SC”/”blood circulation” interface, a SpectraPor® dialysis membrane (MWCO 50 kDa) was installed. To set up the experiments, both “blood circulation” chambers were filled with 75 mL of PBS (pH 7.4), and the “SC” chamber was filled with 7.5 mL of an O/W emulsion composed of lecithin (1.64% w/v, the oil phase) and 1-mg/mL HA/PBS solution (the aqueous phase). ESCAR was placed at 34 °C in a convection chamber, and mild magnetic stirring was applied in both the “blood circulation” chambers. Notably, no stirring was applied in the “SC” chamber, and griseofulvin was reported to have limited binding/adsorption (< 5%) to the ESCAR surfaces (22). For all experiments, the suspension injection volume was kept at 1.5 mL, and drug concentration in suspension was adjusted according to the pre-determined doses. The suspension was slowly injected from the injection port into the central region of the “SC” chamber using a 3-mL syringe connected with a 23G × 3/4 needle (BD, NJ, USA).

Before 8 h, at each time point, 1.5 mL of aliquots (0.75 mL for each “blood circulation” chamber) were withdrawn with the replacement of 1.5 mL of PBS. At the 8-h time point and beyond, to maintain the concentration gradient and keep drug concentrations in the “blood circulation” chambers low, 100 mL of liquid (50 mL for each “blood circulation” chamber) was withdrawn with the replacement of the same volume of PBS. For each dose/formulation combination, the release test was carried out in triplicate.

Results and Discussion

Suspension Settling

Turbidity was caused by suspended particles and therefore was used as an indicator to describe the extent of particle settling. Figure 2 presented the normalized absorbance values of the unmilled and milled suspensions versus time. As shown, the absorbance of unmilled particles declined more rapidly compared to that of milled particles, for example, (i) at 1 h, ~ 20% decline for the milled suspension *vs.* ~ 55% decline for the unmilled suspension. (ii) at 3 h, ~ 50% decline for the milled suspension *vs.* ~ 70% decline for the unmilled suspension. These results indicated that the unmilled particles (d_{50} of unmilled suspension 26.2 μ m) settled faster than the milled particles (d_{50} of milled suspension 1.5 μ m).

Drug Permeation Tests to Determine k_{mem}

Drug permeation through a 50 kDa-MWCO membrane was measured using a side-by-side cell, with the results shown in Fig. 3a. As seen, from 10 to 100 min, the concentration in the donor cell had a linear decrease by ~7.5%, whereas the concentration in the receiver cell increased linearly by ~4 times. The linear change of the concentrations in the donor and receiver cells indicated a steady-state flux. Based on the values listed in Table I, using Eq. 7, the permeability constant k_{mem} was calculated to be 2.951E–1 cm/h.

Membrane Flux Tests to Determine k_P

The tests aimed to study the effect of the lecithin phase (1.64%w/v) on drug partition and determine the partition constant k_P, as it was presumed that (i) in an o/w emulsion system, a certain amount of drug molecules would partition in the dispersed oil phase; (ii) drug partition in both the oil and aqueous phases maintained a dynamic equilibrium; (iii) the oil phase occupied a small volume and was unlikely to contact or have good affinity with the membrane. Therefore, only drug molecules in the continuous aqueous phase could permeate through the membrane. As shown in Fig. 3b, for both groups, the permeated drug amount increased linearly as a function of time but exhibited different slopes. According to Eq. 10, k_P was the ratio of two slopes and was calculated to be 3.145. This result suggested that griseofulvin had a higher partition in the oil phase compared to the aqueous phase, which was in agreement with the lipophilic property of griseofulvin.

Drug Release in ESCAR

Drug release tests were carried out for the unmilled and milled suspensions. The experimental drug release data were presented in Fig. 4, shown as the discrete data points. It

is worth mentioning that the data of four dose/formulation combinations were obtained from Fig. 3 in our previous paper (22).

Drug release in ESCAR is a multi-step process: (i) drug molecules dissolve from particles; (ii) drug molecules rapidly diffuse and partition in the aqueous and oil phases; (iii) some drug molecules that reside in the aqueous phase and nearby the membranes have a chance to permeate through the membranes and then release to the “blood circulation” chambers. Steps (i) and (III) were considered as two rate-limiting steps of drug release. Considering step (i), since griseofulvin is poorly water-soluble (10 μ g/mL in PBS reported by Chiang *et al.* (8)) particle micronization was used to enhance the dissolution rate (23–25). As seen, at 102 h, the milled suspensions (Fig. 4a) presented higher drug release compared to the unmilled suspensions (Fig. 4b) across all doses, and the effect of particle micronization on drug release enhancement was more obvious at the low dose(s). For example, regarding the drug release of the 1.5-mg dose, compared to the unmilled suspension, the milled suspension was higher with (i) 54% at 8 h; (ii) 44% at 30 h; (iii) 44% at 66 h; (iv) 48% at 102 h. In contrast, regarding the drug release of the 36-mg dose, compared to the unmilled suspension, the milled suspension was higher with (i) 13% at 8 h; (ii) 13% at 30 h; (iii) 12% at 66 h; (iv) 10% at 102 h. Hence, the effect of particle micronization on drug release enhancement was diminished if higher doses were used. Furthermore, for the unmilled suspensions, the higher doses substantially increased drug release, e.g., when increasing the dose from 4.5 mg to 36 mg, drug release increased by 79% at 102 h. On the contrary, the dose effect was less noticeable for the milled suspensions, e.g., when increasing the dose from 4.5 mg to 36 mg, drug release only increased by 11% at 102 h.

Furthermore, using the IVIVC model developed in our previous study (22), the rat PK profiles could be simulated from the *in vitro* drug release profiles. Some simulated PK results were shown in Fig. S1 of the Supporting Information.

Drug Release Modeling

The parameters for drug release model development were listed in Table II. According to the experimental data (shown in Fig. 4), drug release rates were observed to be relatively constant between 0 and 8 h, between 8 and 30 h, and between 30 and 102 h. Hence, to simplify the model, $Q_{(t,\mathrm{Dia,Dose})}$ was assigned to three constant values for these three timeframes respectively. By solving Eqs. 1, 4, and 6, the experimental data were fitted by the model, shown as the dashed lines in Fig. 4. The R^2 values, summarized in Table III, were all higher than 0.99, indicating that the best-fit model could predict the experimental data across all doses and formulations. It was worth pointing out that $CF_{(t,\mathrm{Dia,Dose})}$ was a required parameter for the model. The model without $\mathrm{CF}_{(t,\mathrm{Dia.Dose})}$ could not fit the experimental data (presented in Fig. S2 of the Supporting Information). Figure 5 showed the aqueous phase concentration in Compartment 1 (Conc1) versus time. As seen in Fig. 5a, for the milled suspensions, from 0 to 8 h, Concl were similar and greater than 0.8 of griseofulvin solubility (> 8 μg/mL) for all doses. In the contrast, in Fig. 5b, for the unmilled suspensions, Concl became higher as doses increased, e.g., ~8.5 μg/mL of the 36-mg dose *vs*~6.5 μg/mL of the 1.5-mg dose. After 8 h, mainly due to particle settling, Concl dropped rapidly, and the high doses could maintain a relatively higher Concl compared to the low doses.

Furthermore, Fig. 6 showed that, for both unmilled and milled suspensions, the best-fit $Q_{(t,\text{Dia,Dose})}$ could follow a power function of dose, given the fact that all the R^2 values were higher than 0.96. Hence, the $Q_{(t,\text{Dia, Dose})}$ value of other doses could be predicted from the developed power function, and then their drug release profiles could be simulated by solving Eqs. 1, 4, and 6. As seen in Fig. 6, the $Q_{(t,\text{Dia,Dose})}$ values of the 0–8 h timeframe were at least one order of magnitude larger than those of the 30–102 h timeframe, implying that more particle settling over time profoundly lowered drug dissolution. The particle settling effect was dose dependent. Based on Eq. 6, a higher dose would enlarge the total theoretical surface area by N_0 times. However, $Q_{(t,\text{Dia,Dose})}$ became a smaller value as the dose increased. In consequence, the particle settling effect could offset the dose effect. In addition, the $Q_{(t,\text{Dia,Dose})}$ values of the unmilled suspension were approximately one order of magnitude larger than those of the milled suspension, indicating particle settling had more effect on slowing the drug release of the milled suspensions. Therefore, the benefits of particle micronization on enhancing dissolution rate could be substantially minimized by particle settling, especially when high doses were used.

According to our developed model, various input parameters can potentially affect drug release and the $Q_{(t,\text{Dia,Dose})}$ values and therefore worth to be studied in our future work. Nanosuspensions can be prepared by various milling techniques/instruments such as rotor–stator, wet media mill, etc. (26) If the preconditions satisfy that milled particles have narrow size distributions and nearly spherical shape, the model can possibly fit and simulate drug release profiles based on different values of Dia_0 and N_0 in Eq. 5. In addition, drug release might be affected by compound aqueous solubility and hydrophobicity, which are related to C_s and k_P (V_d) in Eq. 6 and thereby can be predicted by the model. Furthermore, combined with the IVIVC model, using ESCAR with proper release medium might aid understanding the influences of some potential patient dosing regimens such as injection volume, dosing frequency, injection site, etc.

Conclusion

In this study, the drug release behavior of both unmilled and milled suspensions was investigated in ESCAR. The experimental data could be predicted by a mass transport-based drug release model. A correction factor $Q_{(t,\text{Dia,Dose})}$ was implemented in the developed model. It was found that the relationship of $Q_{(t,\text{Dia,Dose})}$ and dose followed a power function. Therefore, for new dose(s), their $Q_{(t,\text{Dia,Dose})}$ values could be predicted. Next, by inputting the $Q_{(t,\text{Dia,Dose})}$ value into Eq. 6, the simulated drug release profiles could be obtained. Ultimately, with these in-silico drug release data, in vivo PK profiles could be simulated using the IVIVC model proposed in our previous study (22).

Supplementary Material

Refer to Web version on PubMed Central for supplementary material.

Acknowledgements

The authors thank Mr. Ryan Grigsby for his support. The authors thank KU Nanofabrication Facility for providing the necessary resources. The authors also thank the support from NIH P30GM145499.

References

1. Dubbelboer IR, Sjögren E. Overview of authorized drug products for subcutaneous administration: pharmaceutical, therapeutic, and physicochemical properties. Eur J Pharm Sci. 2022;173:106181. [PubMed: 35381330]
2. Flexner C, Owen A, Siccardi M, Swindells S. Long-acting drugs and formulations for the treatment and prevention of HIV infection. Int J Antimicrob Agents. 2021;57(1):106220. [PubMed: 33166693]
3. Chen W, Yung BC, Qian Z, Chen X. Improving long-term subcutaneous drug delivery by regulating material-bioenvironment interaction. Adv Drug Deliv Rev. 2018;127:20–34. [PubMed: 29391221]
4. Lynch PM, Butler J, Huerta D, Tsals I, Davidson D, Hamm S. A Pharmacokinetic and tolerability evaluation of two continuous subcutaneous infusion systems compared to an oral controlled-release morphine. J Pain Symptom Manage. 2000;19(5):348–56. [PubMed: 10869875]
5. Jones GB, Collins DS, Harrison MW, Thyagarajapuram NR, Wright JM. Subcutaneous drug delivery: an evolving enterprise. Sci Transl Med. 2017;9(405):eaaf9166. [PubMed: 28855399]
6. Mathaes R, Koulov A, Joerg S, Mahler H-C. Subcutaneous injection volume of biopharmaceuticals —pushing the boundaries. J Pharm Sci. 2016;105(8):2255–9. [PubMed: 27378678]
7. Sigfridsson K, Lundqvist A, Strimfors M. Subcutaneous administration of nano- and microsuspensions of poorly soluble compounds to rats. Drug Dev Ind Pharm. 2014;40(4):511–8. [PubMed: 23557177]
8. Chiang P-C, Nagapudi K, Fan PW, Liu J. Investigation of drug delivery in rats via subcutaneous injection: case study of pharmacokinetic modeling of suspension formulations. J Pharm Sci. 2019;108(1):109–19. [PubMed: 29909029]
9. Chiang P-C, Ran Y, Chou K-J, Cui Y, Wong H. Investigation of utilization of nanosuspension formulation to enhance exposure of 1,3-dicyclohexylurea in rats: preparation for PK/PD study via subcutaneous route of nanosuspension drug delivery. Nanoscale Res Lett. 2011;6(1):413. [PubMed: 21711942]
10. Sigfridsson K, Rydberg H, Strimfors M. Nano- and microcrystals of griseofulvin subcutaneously administered to rats resulted in improved bioavailability and sustained release. Drug Dev Ind Pharm. 2019;45(9):1477–86. [PubMed: 31260340]
11. Sigfridsson K, Xue A, Goodwin K, Fretland AJ, Arvidsson T. Sustained release and improved bioavailability in mice after subcutaneous administration of griseofulvin as nano- and microcrystals. Int J Pharm. 2019;566:565–72. [PubMed: 31181305]
12. Li D, Chow PY, Lin TP, Cheow C, Li Z, Wacker MG. Simulate SubQ: the methods and the media. J Pharm Sci. 2021 (In Press).
13. McDonald TA, Zepeda ML, Tomlinson MJ, Bee WH, Ivens IA. Subcutaneous administration of biotherapeutics: current experience in animal models. Curr Opin Mol Ther. 2010;12(4):461–70. [PubMed: 20677097]
14. Thomas VA, Balthasar JP. Understanding inter-individual variability in monoclonal antibody disposition. Antibodies. 2019;8(4):56. [PubMed: 31817205]
15. Gao GF, Ashtikar M, Kojima R, Yoshida T, Kaihara M, Tajiri T, et al. Predicting drug release and degradation kinetics of long-acting microsphere formulations of tacrolimus for subcutaneous injection. J Control Release. 2021;329:372–84. [PubMed: 33271202]
16. Gao GF, Thurn M, Wendt B, Parnham MJ, Wacker MG. A sensitive in vitro performance assay reveals the in vivo drug release mechanisms of long-acting medroxyprogesterone acetate microparticles. Int J Pharm. 2020;586:119540. [PubMed: 32590096]
17. Kinnunen HM, Sharma V, Contreras-Rojas LR, Yu Y, Alleman C, Sreedhara A, et al. A novel in vitro method to model the fate of subcutaneously administered biopharmaceuticals and associated formulation components. J Control Release. 2015;214:94–102. [PubMed: 26210441]

18. Bown HK, Bonn C, Yohe S, Yadav DB, Patapoff TW, Daugherty A, et al. In vitro model for predicting bioavailability of subcutaneously injected monoclonal antibodies. J Control Release. 2018;273:13–20. [PubMed: 29355621]

19. Bock F, Lin E, Larsen C, Jensen H, Huus K, Larsen SW, et al. Towards in vitro in vivo correlation for modified release subcutaneously administered insulins. Eur J Pharm Sci. 2020;145:105239. [PubMed: 31987985]

20. Leung DH, Kapoor Y, Alleyne C, Walsh E, Leithead A, Habulihaz B, et al. Development of a convenient in vitro gel diffusion model for predicting the in vivo performance of subcutaneous parenteral formulations of large and small molecules. AAPS PharmSciTech. 2017;18(6):2203–13. [PubMed: 28070846]

21. Torres-Terán I, Venczel M, Klein S. Prediction of subcutaneous drug absorption - do we have reliable data to design a simulated interstitial fluid? Int J Pharm. 2021;610:121257. [PubMed: 34737015]

22. Lou H, Hageman MJ. Development of an in vitro system to emulate an in vivo subcutaneous environment: small molecule drug assessment. Mol Pharm. 2022;19(11):4017–25. [PubMed: 36279508]

23. Rasenack N, Müller BW. Dissolution rate enhancement by in situ micronization of poorly water-soluble drugs. Pharm Res. 2002;19(12):1894–900. [PubMed: 12523671]

24. Rasenack N, Müller BW. Micron-Size drug particles: common and novel micronization techniques. Pharm Dev Technol. 2004;9(1):1–13. [PubMed: 15000462]

25. Rasenack N, Steckel H, Müller BW. Preparation of microcrystals by in situ micronization. Powder Technol. 2004;143–144:291–6.

26. Malamatari M, Taylor KMG, Malamataris S, Douroumis D, Kachrimanis K. Pharmaceutical nanocrystals: production by wet milling and applications. Drug Discovery Today. 2018;23(3):534–47. [PubMed: 29326082]

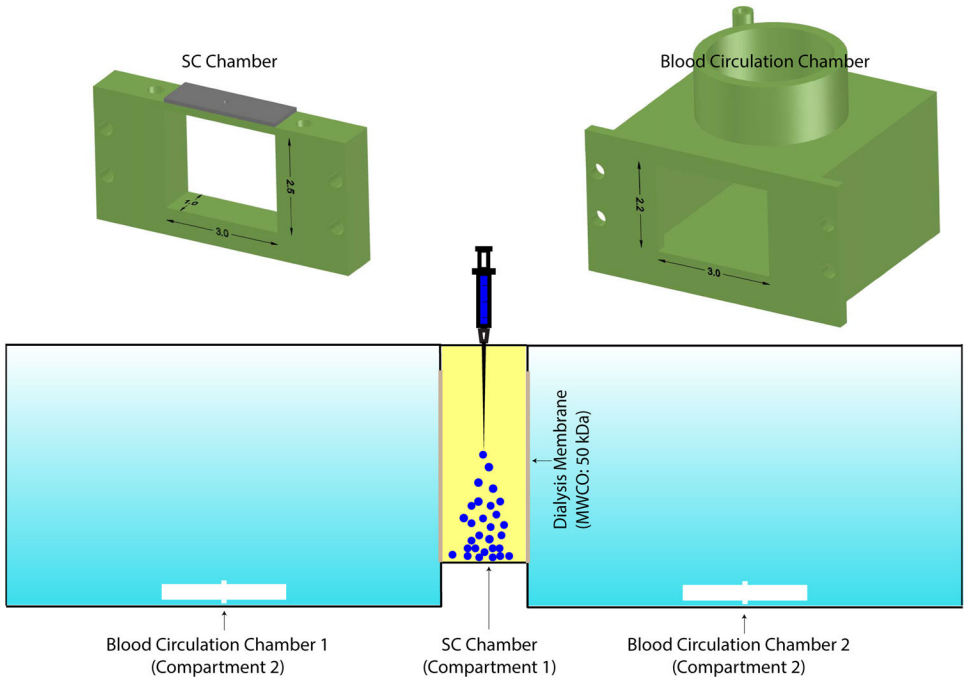

Fig. 1.

ESCAR geometry: one “SC” chamber (Compartment 1) and two “blood circulation” chambers (Compartment 2)

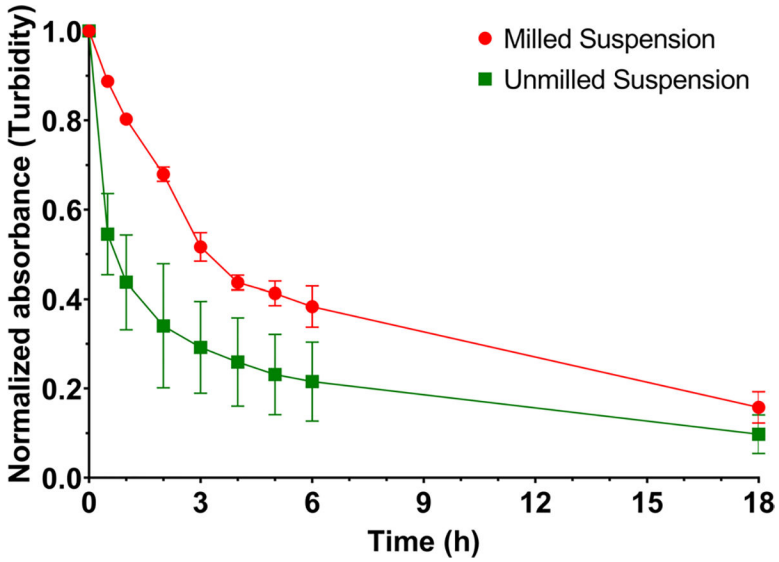

Fig. 2.
Turbidity measurement versus time for the milled and unmilled suspensions

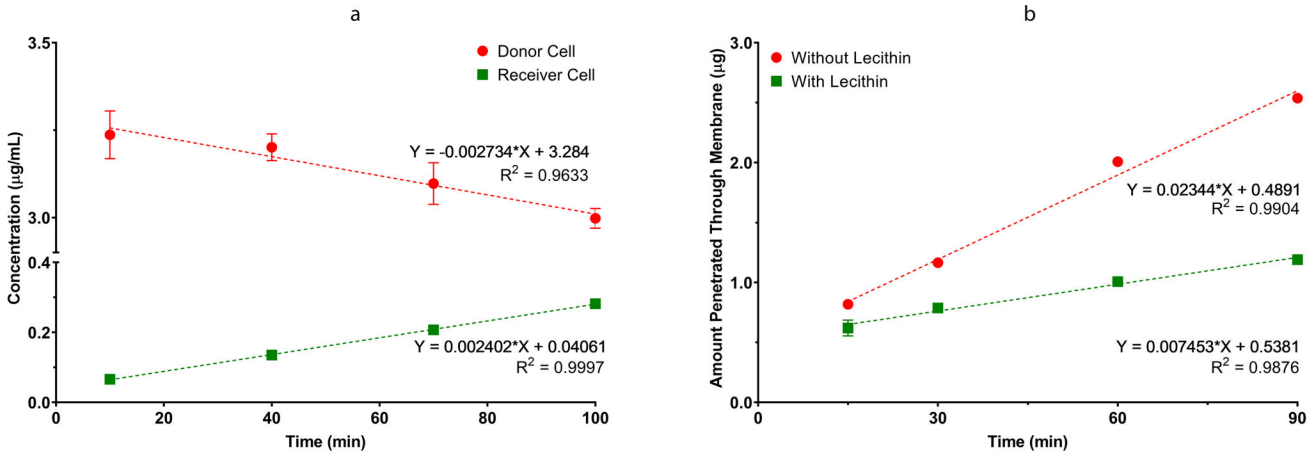

Fig. 3.

a Drug concentration versus time profiles in the donor and receiver cells (the data of the drug permeation tests in "Drug permeation tests to determine k_{mem}" section). **b** Drug amount permeated through membrane versus time profiles with and without lecithin in tests in the donor cell (the data of the membrane flux tests in "Membrane flux tests to determine k_P" section)

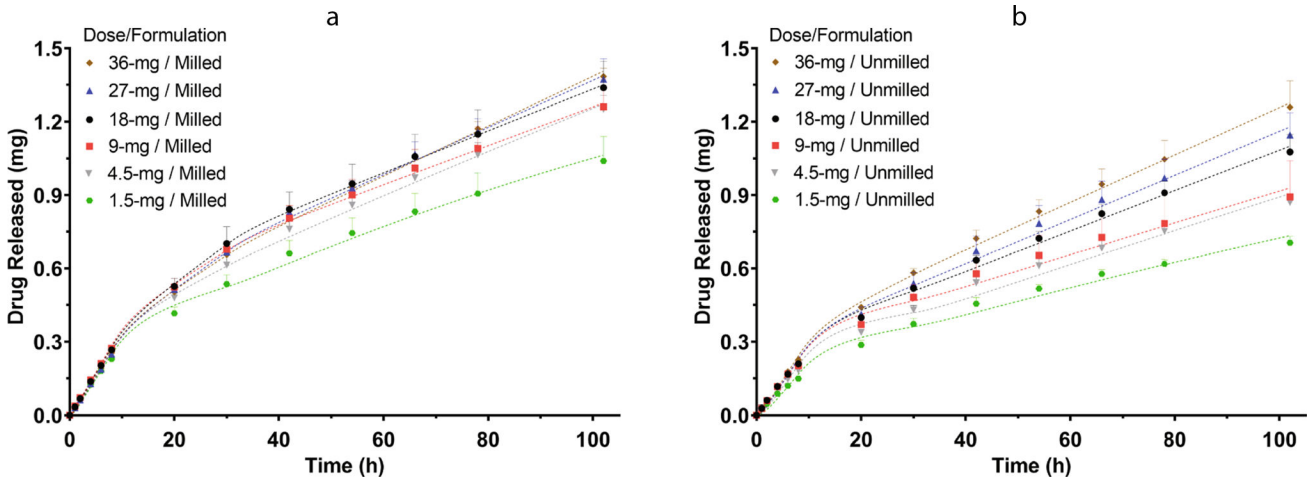

Fig. 4.

Drug release profiles of **a** milled suspensions at different doses; **b** unmilled suspensions at different doses. Experimental drug release data are displayed as discrete data points. Predicted drug release data are displayed as dotted lines

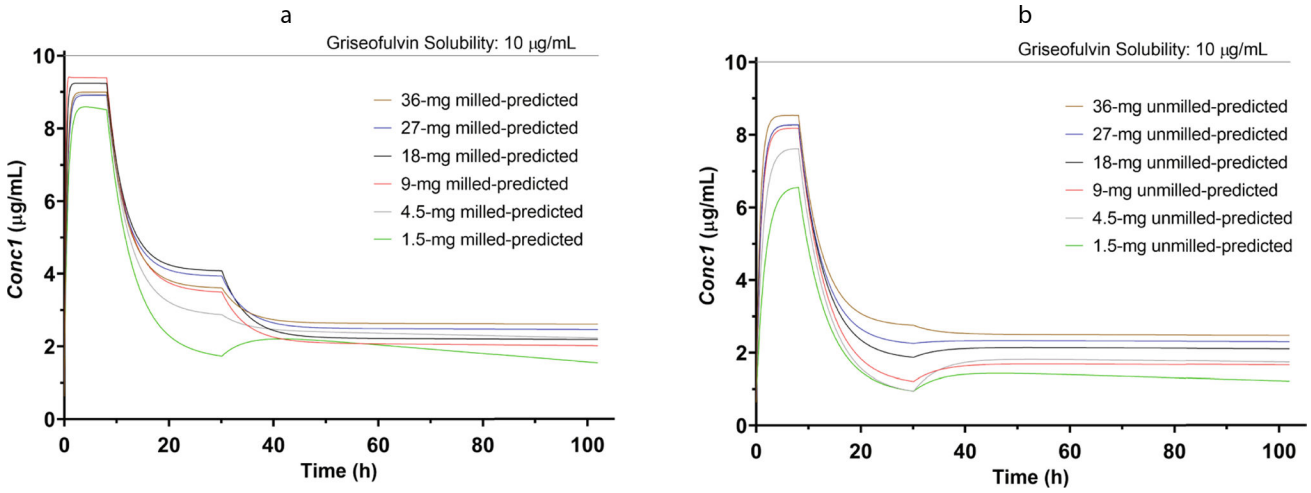

Fig. 5.

The predicted aqueous phase concentration in Compartment 1 (Conc1) profiles of **a** milled suspensions at different doses; **b** unmilled suspensions at different doses

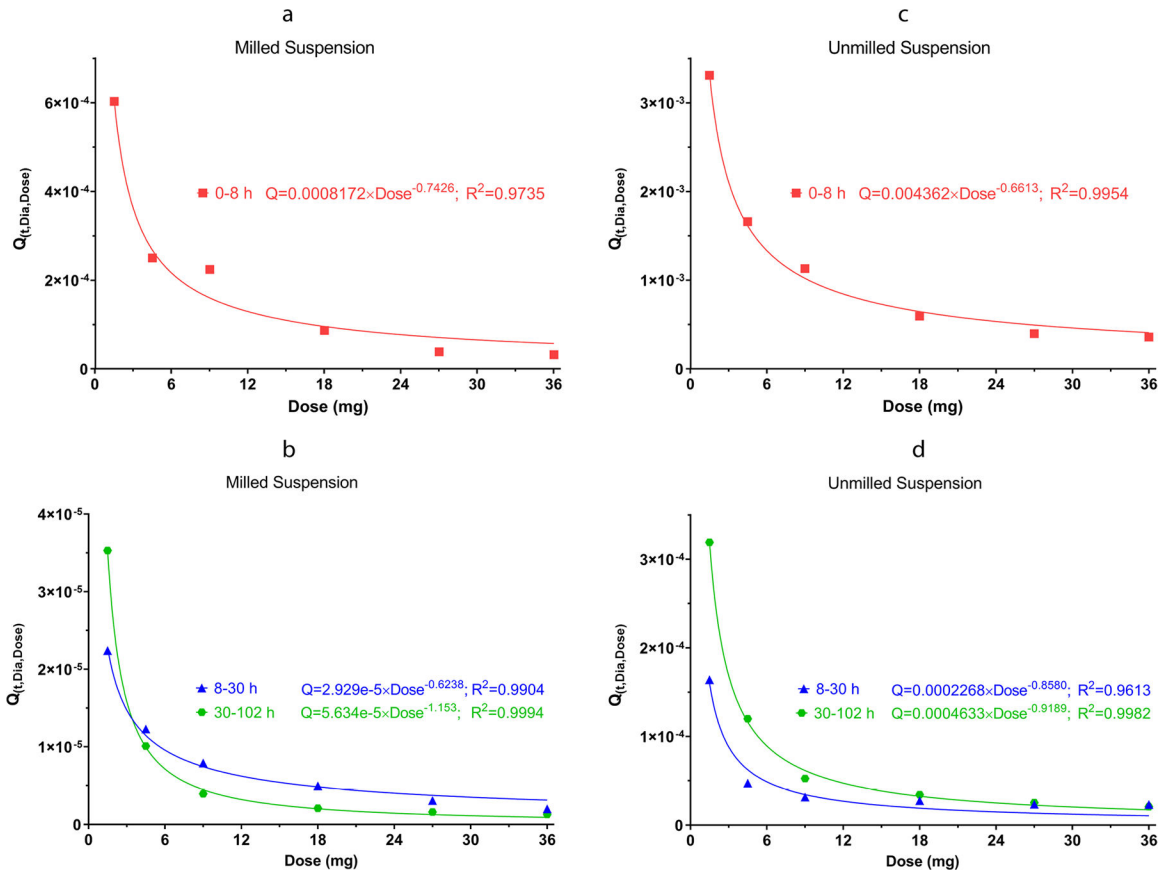

Fig. 6.

The $Q_{(t,\,\mathrm{Dia,Dose})}$ value versus dose that is fitted with a power function. **a** 0–8 h of the milled suspension. **b** 8–30 h and 30–102 h of the milled suspension. **c** 0–8 h of the unmilled suspension. **d** 8–30 h and 30–102 h of the unmilled suspension

Table I

Values of Parameters for Determining the Permeability Constant k_{mem}

SA_{mem} (cm^2)	1.767
V_{donor} (cm^3)	10
$V_{receiver}$ (cm^3)	10
Δt (min)	90
$Conc_{donor}^{10-min}\left(\mu g/cm^3\right)$ *	3.257
$Conc_{donor}^{100-min}\left(\mu g/cm^3\right)$ *	3.011
$Conc_{receiver}^{10-min}\left(\mu g/cm^3\right)$ *	0.0646
$Conc_{receiver}^{100-min}\left(\mu g/cm^3\right)$ *	0.281
k_{mem} (cm/s)	8.197E - 5
k_{mem} (cm/min)	4.918E - 3
k_{mem} (cm/h)	2.951E - 1

* Value obtained by the fitted linear equations

Table II

Parameter Values for Developing Drug Release Models with the Best-Fit Values of $Q_{(t,\mathrm{Dia,Dose})}$

$SA_{\mathrm{permeation}}$	13.2 cm^2
k_{mem}	2.951E – 1 cm/h (obtained from “Drug permeation tests to determine k_{mem}” section)
k_p	3.145 (obtained from “Membrane flux tests to determine k_{p}” section)
V_p	7.5 mL
V_d	23.5875 mL
Dia_0	1.5 μm of the milled suspension; 26.2 μm of the unmilled suspension
$\mathrm{Conc1}_0$	0.636 μg/mL
C_s	10 μg/mL: reported by Chiang *et al.* (8)
ρ	1.3 g/mL: reported by Chiang *et al.* (8)
$Q_{(t,\mathrm{Dia,Dose})}$	Obtained by fitting the experimental drug release data

Table III

R^2 Values for Drug Release Modeling of Multiple Formulation/Dose Combinations

Dose (mg)	R^2 value	
	Milled suspension	Unmilled suspension
1.5	0.9966	0.9918
4.5	0.9986	0.9915
9	0.9994	0.9921
18	0.9997	0.9971
27	0.9994	0.9964
36	0.9992	0.9987